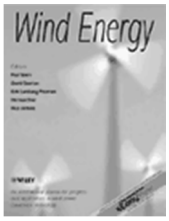

Integrated Offshore Wind Farm Design

Journal:	*Wind Energy*
Manuscript ID	Draft
Wiley - Manuscript type:	Research Article
Date Submitted by the Author:	n/a
Complete List of Authors:	Marge, Thomas; The Johns Hopkins University, Applied Mathematics and Statistics Lumbreras, Sara; Universidad Pontificia Comillas, Institute for Research in Technology Ramos, Andres; Universidad Pontificia Comillas, Institute for Research in Technology Hobbs, Benjamin F.; Johns Hopkins University, Department of Mechanical Engineering \& Center for Environmental and Applied Fluid Mechanics
Keywords:	cable layout, turbine micrositing, wake modeling, economics, offshore wind

Integrated Offshore Wind Farm Design: Optimizing Micrositing and Cable Layout Simultaneously

Thomas Marge, *Johns Hopkins University*
Sara Lumbreras, Andrés Ramos, *Comillas Pontifical University*
Benjamin F. Hobbs, *Johns Hopkins University*

***Abstract*— Electrical layout and turbine placement are key design decisions in offshore windfarm projects. Increased turbine spacing minimizes the energy losses caused by wake interactions between turbines, but requires costlier cables with higher rates of failure. Simultaneous micrositing and electrical layout optimization is required to realize all possible savings. The problem is complex, because electrical layout optimization is a combinatorial problem and the computational fluid-dynamics calculations to approximate wake effects are impossible to integrate into classical optimization. This means that state-of-the-art methods do not generally consider simultaneous optimization and resort to approximations instead.**

We extend an existing model, which successfully optimizes cable design, to consider micrositing simultaneously. We use Jensen's equations to approximate the wake effect in an efficient manner, calibrating it with years of mast data. The wake effects are pre-calculated and introduced into the optimization problem. We solve simultaneously turbine spacing effects and cable layout, exploiting the tradeoffs between these two objectives. We use the Barrow Offshore Windfarm as a case study to demonstrate realizable savings up to 8.8 M EUR over the lifetime of the plant. In addition, the model provides insights on the effects of turbine spacing that can be used to simplify the design process or to support negotiations for surface concession at the earlier stages of a project.

Keywords*—Offshore wind, economics, wake modeling, turbine micrositing, cable layout*

THE Paris Agreement, currently ratified by 142 countries, aims to limit global warming over the next hundred years to 1.5 degrees [1,2]. In order to meet these aggressive targets, the European Union must reduce carbon by 20% by 2020 and by 80% by 2050 [2]. In Europe, offshore wind farms have a promising future, especially in the Irish, Baltic, and North seas where shallow waters provide inexpensive access to consistent, substantial wind resources [3]. These changes are economically feasible and have substantial financial support [2,4]. 10.3 GW of new European wind power capacity were financed in 2016 alone [5]. While there are still significant technological and economic barriers, it is feasible for the United States to achieve 20% or more of its energy from wind supply [6]. As onshore space becomes scarce, offshore windfarm technology has become essential to meet these targets in both Europe and the United States [7].

Decisions about the location of offshore farms (macrositing) [8-10], specific turbine placement in the layout (micrositing) [10-12], and electrical design [10] are all problems faced by offshore windfarm development. Electrical design is closely tied to micrositing and accounts for approximately 20% of project costs [13], so it is a relevant consideration in windfarm layout design. In addition, offshore windfarms have higher repair times and costs than their onshore counterparts, so failure rate modeling is also an important consideration when determining layouts [10,14,15].

This paper investigates the benefits that can be achieved by integrating turbine placement optimization concurrently with cable layout design. The contributions of this paper are the following:

- It proposes a method to calibrate the wake-effect description of the model in an efficient manner, based on clustering years of mast data.
- It proposes a method to consider simultaneously both effects.

- It presents the extension to a previous model called OWL (Offshore Windfarm Layout Model) [10], for simultaneously optimizing micrositing and cable layout.
- It carries out a real case study based on Barrow Offshore Wind Farm (BOWF), which demonstrates the high potential savings associated with concurrent optimization.
- It provides insight on the tradeoffs associated to turbine spacing and wake effects. This information can be used to simplify the design process or the support negotiations for surface concession at the earlier stages of a project.

This article is organized as follows. First, a brief review of existing offshore windfarm design models is presented in Section I. Then, candidate modeling methodologies are discussed, with a focus on wake effects (Sections II, III). The developed model and case study are then described (Sections IV, V). Finally, results are presented and conclusions offered (Sections VI, VII).

I. Literature Review

Here we summarize the state of the art for addressing the two problems that are simultaneously solved by the developed model: turbine placement (known as micrositing) and cable layout. Cable layout costs can represent approximately 20% of the costs of wind farm installation, and can vary between layout choices by approximately 10%. Savings associated with the wake effect similarly vary by approximately 2% of the total cost of projects, giving it a similar magnitude impact on the project as cable costs.

A. *Turbine Placement*

Turbine placement optimization, also known as micrositing, deals with the tradeoff between energy production and investment cost as turbine configurations are changed. At the most basic level, it accounts for the energy loss generated by the wake effect in comparison to the cost of spacing turbines further apart. Electrical component installation, surface concession, and environmental impact may all be relevant to this calculation [16]. Existing micrositing models usually focus on maximizing energy production while constraining to farm construction budgets, maximizing a definition of profit or minimizing energy cost [17].

All fluid dynamics models found in the literature are based on Katic's refinement of Jensen's model as described in reference [18] because of its simplicity and accuracy. Models may [19] or may not [20] consider wind direction and wake effect variation.

Most methods for optimizing turbine placement consider expansions and contractions of standard layouts. Some models test several standard configurations, and compare the optimal spacing for each configuration [21]. Classical Mixed-Integer Programing has been employed to solve this problem up to optimality [22,23]. However, a large range of metaheuristic techniques have also been employed, including multi-objective evolutionary algorithms [16,24], gradient search [17,24], greedy heuristics [17,24], Genetic Algorithms [17,21,24-26], Simulated Annealing [17,20,24], Particle Swarm Optimization [19] and pattern-search algorithms [17,24]. Only a very reduced subset of these works considers non-conventional layouts [20,27].

Electrical-layout installation costs are crucial when considering variable turbine spacing [16]. However, most models resort to simple heuristics for an approximation of cable layout costs, with the minimum-spanning tree being the most popular [16].

To the best of our knowledge, there are no previously published models that deal simultaneously with micrositing and cable layout without resorting to simplifications or standard configurations. However, our model still lacks the generality of some heuristic turbine spacing models [20,27], because the model requires finitely many turbine placement layouts to be prespecified as input. Wake-effect costs are not well approximated linearly, so any Mixed-Integer Linear Programming (MILP) model must select which turbine configurations will be considered pre-optimization so that wake costs can be pre-calculated for each layout.

B. *Electrical Layout Optimization*

The importance of the electrical layout in offshore wind farms has motivated the application of a wide array of techniques. A complete survey can be found in reference [28]. The electrical layout is comprised of two parts: the collector system (which links the wind turbines among them), and the transmission system (that takes the power to the point of common coupling in the onshore grid). The options considered for the collector system are generally reduced to standard designs [10,13,28-30], such as stars, single-sided rings, double-sided rings, radial layouts and multi-rings. However, the optimal layout has a strong dependency on the precise layout of turbines, which greatly influences installation costs and failure rates. As a result, standard configurations are rarely optimal [10,31]. Only a few works allow for flexible designs, but this is done at the expense of using heuristic techniques for layout design rather than classical optimization[10,32,33].

Reliability is a very important factor in layout design, as repairs offshore are difficult and costly. Failures can be approximated deterministically [34,35], modelled as scenarios in a stochastic program [31,36] or simulated [37,38]. However, most models ignore its effects [39,40].

The transmission system is responsible for sending generated power to the point of common coupling with the electrical grid. Several options exist for this transmission [41]:

- MVAC, for small amounts of power being transmitted short distances.
- HVAC, which elevates voltage using a transformer [11,40]. As volume of power and distance to shore increase, so do the losses. This is currently the most common solution [42], but is expected to become less common if farm sizes continue to increase and move away from shore.
- HVDC, which enables more efficient transmission of large amounts of power over greater distances [29,43,44]. It also allows for connection to weaker grids [40]. HVDC transmission is considered in a few existing models [12,41].

Different modelling compromises can be chosen with respect to power flow calculations. Transportation modeling [31,36], DCLF [35,45] and ACLF [40,46] methods for calculating power flows can all be used. In all models, losses can be ignored [35,45] or approximated by linear or quadratic functions [36,47]. ACLF implementations usually approximate losses.

The cable layout problem can be solved as a classical MILP by representing losses using linear approximations [10], and decomposition strategies can be used for computational savings [10,31,48]. Non-classical strategies such as heuristics [49], Genetic Algorithms [50] or Immune System Algorithms [50] have also been applied in this setting.

II. Methods: Integrating Electrical Layout and Turbine Placement

The model presented in this paper is a MILP that allows for the simultaneous optimization of turbine placement and cable layout, considering flexible configurations and stochastic failures, resorting to classical optimization to guarantee global optimality (see section IV). The model builds on the model developed in reference [10], which optimized cable layout taking turbine placement as an input. The objective function weighs investment cost against the cost of energy lost due to wake effects and cable failures. This calculation is based on relative turbine and substation coordinates for each farm, as well as years of mast data for the site under consideration.

Wake effects were introduced using Jensen's model as applied to entire wind farms in reference [51]. The model is equipped to consider complex wind-rose data from any number of directions at any number of velocities. The model automatically determines which wind scenarios to consider (the scenario-tree centroids) and how to weight (probability) each wind scenario by using the k-means algorithm [52]. This simplified data is then used to determine the wake cost component of the objective function for each turbine placement option being considered. This turbine placement selection is introduced as a new variable in the layout optimization problem.

The reliability of these layouts is considered using scenarios in which each component fails [53] based on calculations of failure and repair rates assuming a discrete Markov process [10]. Multiple

components failing simultaneously is not considered by the model. The model is flexible enough to account for surface concession costs associated with each turbine layout if necessary.

III. Wake Modeling

Wake effects modify the power output produced at each turbine. In order to take them into account, the model takes years of mast data on the scale of minutes, and turns them into a representative wind rose that can be used for the more intensive Jensen model calculations for each turbine.

Micrositing options are modeled through a set of discrete variables that define the spacing among turbine rows and the distance between two consecutive turbines in a row. For each spacing option, the relative distances between turbines are calculated. Then, the model creates a large number of wind-speed and wind-direction bins. Mast data is then used to calculate the appropriate wind speed and direction values for each bin associated to the specific placement considered. For each wind speed bin, the weights for the corresponding wind direction bins are aggregated. Jensen's model is run on all wind direction bins, so that each turbine has an approximated power output for each wind direction bin. The power outputs for each turbine are then combined in a weighted sum to approximate power output for each turbine for each wind direction and speed bin. For a turbine under a given wind speed and wind direction scenario, Jensen's model is calculated as follows:

The local speed deficit for a turbine caused by the wake of another turbine is approximated as in [51]. Let δ be local speed deficit, C_t is the thrust coefficient, r_r is the rotor radius, k_w is the wake decay coefficient, and the turbines are at a distance x from each other.

$$\delta = \frac{1 - \sqrt{1 - C_t}}{(1 + k_w x / r_r)^2}$$

The total wind speed deficit for a turbine based on the deficit coefficients imposed on it by the turbines in whose wake it falls is then calculated as in [51] using the quadratic sum of the square of local speed deficits. Let the turbine under consideration be in the wake of n other turbines:

$$\delta_{total} = \left(\sum_{i=1}^{n} \delta_i \right)^{\frac{1}{2}}$$

The incoming wind velocity is then calculated for each turbine as in reference [51]. Let u_{farm} be the incoming wind velocity to the wind farm and u_{local} be the incoming wind velocity to the turbine.

$$u_{local} = u_{farm}(1 - \delta_{total})$$

The power output for the turbine is then approximated through a linear extrapolation of the two wind-velocity-to-power data points that its velocity falls between. Due to the high number of wind speed bins necessary for precise turbine power calculations, the bins must be condensed into wind speed scenarios. We use K-means clustering [59] to condense these scenarios. The k-means algorithm then clusters windspeed bins with respect to the weight of each bin using the following objective function:

$$kmeans_{obj} = \sum_{i=1}^{n} d_i * min_j(\|p_i - m_j\|)$$

Where n is the number of windspeed bins, d_i is the weight of windspeed bin i, $p_i$is the sum of turbine output power over all turbines in all configurations for windspeed bin i and $m_j$is mean j.

After the k-means algorithm converges, windspeed bins are grouped into scenarios based on the centroid they fall closest to. Power outputs for each turbine for each windspeed scenario are approximated by taking a weighted sum of the power outputs for each turbine over all windspeed bins present in the scenario. Let B be the set of all windspeed bins included in the scenario, p_b be the power output of the turbine for windspeed bin b, d_b be the weight of windspeed bin b and $p_{scenario}$ be the calculated power output of the turbine in the scenario. For a specific turbine in each windspeed scenario:

$$p_{scenario} = \left(\sum_{b \in c} d_b * p_b\right) / \left(\sum_{b \in B} d_b\right)$$

The duration of each windspeed scenario is calculated by taking the sum of the weights of the windspeed bins present in the scenario multiplied by the number of hours in a year. Let α be the duration of a given scenario.

$$\alpha = \left(\sum_{b \in B} d_b\right) * 8.76$$

An ideal turbine power output calculation is also made for each windspeed scenario by calculating the power output for the turbines under that scenario if they were infinitely spaced. Note that all turbines would have the same power output if they were spaced far enough that the wake effects were negligible so long as incoming winds were roughly equivalent everywhere on the windfarm. The energy loss due to the wake effect of a given layout must be considered in two parts of the problem. First, for each layout under consideration, a cost is calculated to account for energy not served by the plant compared to the ideal scenario where turbines experience no wake effect. Second, power not served due to failure is based on power output for each turbine calculated after the wake effect is incorporated.

IV. MILP Model Formulation

The extended OWL model considers multiple input turbine layout proposals and returns the optimal turbine layout or micrositing scheme. In addition, it returns the optimal collector and transmission systems for that offshore wind farm [10]. Turbine layouts are given, together with a pre-specified point of common coupling (PCC) and possible locations for offshore substations. Which cables are to be considered for installation, as well as available cable types, transformers and converters are also specified as inputs. The problem formulation below shows the full formulation of the MILP problem considering both micrositing and cable layout. We list the indices, parameters, decision variables, constraints and the joint objective function.

1) Indices:

a) Configuration of the wind farm

- p, p': geographical points where elements can be placed
- $wt(p), cp(p), ps(p)$: specific geographical points for the turbines, the point of common coupling and the offshore substations
- d: turbine layouts under consideration (e.g. row separation of 1000, 1050, 1100, or 1150 meters)

b) Equipment

- $ct, ctac(ct), ctdc(ct)$: types of cable considered, subset of AC and subset of DC types $vl, vldc(vl), vlwt(vl)$: voltages that can be used, followed by a DC subset and the voltage level of turbines tt: type of transformer or converter
- vs: side of the voltage (upper or lower). This set is used for enforcing voltage consistency.

- r : parallel-element index. If several elements are installed in parallel, having a different value for this index allows to differentiate them.

c) Stochasticity

- ws : scenario for wind input
- ss : scenario for component failure.

In the following sections, a subindex refers to component failures, while a superindex denotes wind input.

2) Parameters:

a) Geometry

- $D_{p,p\prime,d}$: distance between two points [m]

b) Components

- $CP_{ct}, CC_{ct}, CX_{ct}, CR_{ct}, Cl_{ct}, Cm_{ct}$: capacity, investment cost, reactance, resistance, rate of failure and repair [MW, MEUR per km, p.u., p.u., failures per km per year and repairs per year respectively]. The binaries $BCV_{ct,vl}$ summarize the information on what voltage level corresponds to each cable type.
- $TP_{tt}, TC_{ct}, TVL_{tt}, TVH_{tt}, TL_{tt}, Tl_{tt}, Tm_{tt}$: capacity, investment cost, voltage level (lower), voltage level (upper), coefficient for losses, rate of failure and repair [MW, MEUR, kV, kV, p.u., failures per year and repairs per year respectively]. The binaries $BTV_{tt,vs,vl}$ summarize what voltage levels correspond to a transformer or converter type.

c) Financial information

- $CCP, CLoss$: cost of curtailment and losses [MEUR per MWh]
- L, R : useful life and interest rate [years, %]

d) Uncertainty

- $WTP^{ws}_{wt(p),d}$: power generated by a turbine in a scenario [MW]
- $maxturb^{ws}$: maximum power generated by a turbine [MW]
- Dur^{ws}: annual hours that correspond to a wind scenario [h]
- $Prob^{ss}_{d}$: probability of a given component failure [p.u.]
- $FaC^{ss}_{p,p\prime,ct,r,d}$: binary parameter that summarizes whether an element (in this case, a cable) is down on a given state.
- $FaTf^{ss}_{tt,r}$: binary parameter that summarizes whether an element (in this case, a transformer or converter) is down on a given state.

e) Other

- M : 'big M' parameter

3) Variables

a) Design variables, all binary

- vd_{d}: micrositing layout choice
- $vWTP^{ws}_{p/p\in wt(p)}$: use wind turbine power outputs for selected distance
- $v_{p,vl}$: voltage level chosen for a point in the design
- os_{p} : placement of a substation at a point
- $c_{p,p\prime,ct,r,d}$: installation of a cable
- $tf_{p,p\prime,tt,r,vs}$: installation of a transformer or converter station

b) Variables describing operation, all continuous:

- $fc^{ws,ss}_{p,p\prime}$: power flow [MW]
- $q^{ws,ss}_{p}$: voltage angle according to Kirchhoff's Second Law [rad]

- $wtpns_p^{ws,ss}$: curtailment for a turbine [MW]
- $pns^{ws,ss}$: energy deficit with respect to the available power [MW]
- $ps_{p/p\in cp(p)}^{ws,ss}$
- $loss_{p,p\prime}^{ws,ss}$: losses in a line [MW]
- $losstf_{p,p\prime}^{ws,ss}$: losses in a transformer[MW]

4) Constraints

The model enforces the following constraints:

a) Design constraints

- There is only one possible layout:

$$\sum_d vd_d = 1. \tag{1}$$

- Cables must respect the choice of layout:

$$c_{p,p\prime,ct,r,d} \leq vd_d,\ \forall p,p',ct,r,d. \tag{2}$$

- The choice of distance must be consistent with turbine power:

$$vWTP_p^{ws} = \sum_d WTP_{p,d}^{ws} * vd_d \quad , \quad \forall\, p, \frac{d}{p} \in wt(p). \tag{3}$$

- There can be no cables installed in points where there is no other element installed:

$$c_{p,p\prime,ct,r,d} \leq os_p \forall p \notin wt(p), p \notin cp(p). \tag{4}$$

- Same as above, enforced for transformers and converters:

$$os_p \geq \sum_{p\prime,tt,r,vs} tf_{p,p\prime,tt,r,vs}$$

$$\sum_{ct,r\prime,d} c_{p,p\prime,ct,r\prime,d} \geq tf_{p,p',tt,r,vs}\ . \tag{5}$$

- There can only be one transformer or converter type, although there can be elements in parallel:

$$\sum_{tt} tf_{p,p\prime,tt,r_1,vs} \leq 1, \forall p,p',vs$$

$$\sum_{vs} tf_{p,p\prime,tt,r_1,vs} \leq 1, \forall p,p',tt. \tag{6}$$

- Same as above, in the case of cables:

$$\sum_{ct} c_{p,p\prime,ct,r_1,d} \leq 1\ . \tag{7}$$

- Auxiliar constraint to impose that redundancy is defined in ascending order:

$$c_{p,p\prime,ct,r,d} \leq c_{p,p',ct,r',d} \quad tf_{tt,rt} \leq tf_{rt\prime} \quad r \geq r'.$$

(8)

- All nodes have a voltage:

$$\sum_{vl} v_{p,vl}=1.$$

(9)

- Only the transformers that are consistent with the voltage of the node can be installed:

$$\sum_{tt,vs/BTV_{tt,vs,vl}=0} tf_{p,p\prime,tt,r_1,vs} \leq 1 - v_{p,vl}.$$

(10)

- Same as above, expressed for cables:

$$c_{p,p',ct,r_1,d} \leq \sum_{vl/BCV_{ct,vl}=1} \left\{ v_{p,vl} + \sum_{tt,vs,vs'/vs\neq vs'} tf_{p,p',tt,r_1,vs} \left(BTV_{tt,vs',vl} - BTV_{tt,vs,vl} \right) \right\}$$

$$c_{p,p\prime,ct,r_1,d} \leq \sum_{vl/BCV_{ct,vl}=1} \left\{ v_{p,vl} + \sum_{tt,vs,vs'/vs\neq vs'} tf_{p\prime,p,tt,r_1,vs} \left(BTV_{tt,vs',vl} - BTV_{tt,vs,vl} \right) \right\}$$

(11)

Connectivity is imposed by groups. This is not necessary but makes the formulation of the MIP problem *tighter*, reducing the feasible region without compromising optimality, therefore enhancing resolution:

$$\sum_{p',ct,r,d/wt(p)} c_{p,p',ct,r_1,d} \geq 1$$

$$\sum_{p,p',ct,r,d/ps(p),cp(p')} c_{p,p',ct,r,d}\, CP_{ct} \geq card(wt)\overline{WTP}$$

$$\sum_{p,p',tt,r/ps(p),cp(p')} tf_{p,p',tt,r} TP_{tt} \geq card(wt)\overline{WTP} - M\left(1 - \sum_{p,p',tt,r\backslash ps(p),cp(p'),r=1} tf_{p,p',tt,r}\right)$$

(12)

b) Link constraints (which deal with design and operation)

- Definition of power not served:

$$pns^{ws,ss} = \sum_{p/p\in wt(p)} wtpns_p^{ws,ss} \quad \forall\, ws, ss.$$

(13)

- Capacity constraints:

$$fc_{p,p'}^{ws,ss} \le \sum_{ct,r,d} c_{p,p',ct,r,d} \cdot \left(1 - FaC_{p,p',ct,r}^{ws,ss}\right) \cdot CP_{ct}$$
$$fc_{p,p'}^{ws,ss} \ge -\sum_{ct,r,d} c_{p,p',ct,r,d} \cdot \left(1 - FaC_{p,p',ct,r}^{ws,ss}\right) \cdot CP_{ct}$$
$$fc_{p,p'}^{ws,ss} - \overline{WTP} \cdot card(wt) \cdot \left(1 - \sum_{tt,r_1,vs} tf_{p,p',r,vs}\right) \le \sum_{tt,r,vs} tf_{p,p',r,vs} TP_{tt} \cdot \left(1 - FaTf_{p,p',r,vs}^{ss}\right)$$
$$fc_{p,p'}^{ws,ss} + \overline{WTP} \cdot card(wt) \cdot \left(1 - \sum_{tt,r_1,vs} tf_{p,p',r,vs}\right) \ge -\sum_{tt,r,vs} tf_{p,p',r,vs} TP_{tt} \cdot \left(1 - FaTf_{p,p',r,vs}^{ss}\right)$$
$$\forall p, p', ws, ss.$$

(14)

c) Operation constraints:

- Balance of energy (First Kirchhoff's law):

$$\sum_{p'} fc_{p',p}^{ws,ss} + vWTP_{p/\,p\in wt(p)}^{ws} - \sum_{p'} loss_{p',p}^{ws,ss} = +wtpns_{p/p\in wt(p)}^{ws,ss} + ps_{p/p\in cp(p)}^{ws,ss} \cdot$$
$$\forall p, ws, ss.$$

(15)

- Second Kirchhoff's law, which is never applied to DC cables:

$$\sum_{p',p} fc_{p',p}^{ws,ss} \le \frac{\left(\theta_p^{ws,ss} - \theta_{p'}^{ws,ss}\right)}{CX_{ct} \cdot ord(r)} + M \cdot \left(1 - \sum_{r'} c_{p,p',ct,r,d}\right)$$
$$\sum_{p',p} fc_{p',p}^{ws,ss} \ge \frac{\left(\theta_p^{ws,ss} - \theta_{p'}^{ws,ss}\right)}{CX_{ct} \cdot ord(r)} - M \cdot \left(1 - \sum_{r'} c_{p,p',ct,r,d}\right)$$
$$\forall p, p', ct, r, d/r' > r, ws, ss.$$

(16)

5) Objective Function

The total cost of the layout is minimized. The problem considers investment costs, the production deficit due to wake effects, losses and curtailment due to equipment failures:

$$\min \left\{ \frac{R\cdot(1+R)^L}{(1+R)^L - 1} \cdot \left[\sum_{p,p',ct,r,d} c_{p,p',ct,r,d} D_{p,p',d} CC_{ct} + \sum_{tt,r} tf_{tt,r} TC_{tt}\right] + CPP \sum_{ws,ss} Dur^{ws} Prob^{ss} pns^{ws,ss} + \right.$$
$$CPP \sum_{ws} \left(maxturb^{ws} Dur^{ws} card(wt) - \sum_{p/p\in wt(p)} Dur^{ws} vWTP_{p/p\in wt(p)}^{ws}\right) +$$
$$\left. CLoss \sum_{p,p',ss,ws} Dur^{ws} Prob^{ss} \left(loss_{p,p'}^{ws,ss} + losstf_{p,p'}^{ws,ss}\right)\right\}.$$

(17)

Although losses add considerable complexity, they have a limited impact on the layout [10]. We incorporate them by means of a two-phase approximation.[10] This reference[54] discusses a more computationally intensive method for this calculation.

V. Case Study

The windfarm layout optimization model was applied to the Barrow Offshore Windfarm, currently in operation, to demonstrate the potential savings compared to conventional windfarm design techniques. When commissioned by Centrica and Dong Energy in 2006, it was the largest offshore windfarm ever built. Barrow is located in the Irish sea, and it includes 30 Vestas V90-3MW turbines creating a 90MW capacity windfarm [55,56]. The turbines are evenly spaced in 4 rows, two with 7 turbines and two with 8. The voltage of electricity generated is modified by an offshore transformer before transmission to shore. A more detailed account of its components can be found in reference [55].

Our model considers HVAC, MVAC and HVDC transmission systems from two possible offshore

substation locations. The collector system was also simultaneously optimized, unrestricted by classical collector patterns. Anywhere from one to six turbine layouts were considered concurrently, generating between 91 and 546 possible elements to be modeled by the N-1 failure criterion. Each layout considered was represented by its own decision variable. While the considered layouts were scaled versions of the actual Barrow Windfarm Layout, the model is equipped to handle any input turbine layout.

The power curve for the V90-3MW was available for precise power generation estimates for incoming windspeeds approximated by Jensen's model in each scenario [57]. The turbine's diameter is 90m [57]. The wind data used for the Jensen's model calculations was derived from the 75-meter mast located at Shell Flats which was used for the original planning of the windfarm [55]. 211,746 ten-minute wind speed and direction data points were used, representing over a year and a half of data collection [58]. When implementing Jensen's model, the wake expansion coefficient was taken from reference [51], as its methodology proved to be suitable to approximate wake deficit (and thus, energy production) in a simple manner.

The turbine's thrust coefficient was approximated to be constant as in references [59-61]. The thrust coefficient was taken to be 0.78 based on models of the V80 turbine [61], which is similar to the 0.75 used in models of the Holec WPS-30 [51]. No thrust coefficient data was found for the V90. Even though the thrust coefficient diminishes for higher wind velocities, the turbines operate near maximum capacity in this region despite the wake effect. While the thrust coefficient was taken to be constant in the case study, the model is equipped to use non-constant approximations of the thrust coefficient.

The 10-minute windspeed data was split into 200 windspeed bins and 400 wind direction bins, running one Jensen simulation for each windspeed wind direction pair with corresponding mast data points. Wind direction bins are more numerous than windspeed bins because slight changes in wind direction can drastically change the turbine power outputs depending on whether a wake from one turbine hits another. The number of bins necessary was approximated by plotting average windfarm power outputs for an increasing number of bins until the outputs converged to within 1 MW of 32.5 MW. The 80,000 Jensen iterations were then sorted into 20 windspeed scenarios using 5000 k-means iterations. Multiple windspeed scenarios are necessary to ensure that the objective function is properly impacted if low cable power ratings lead to power not served under high wind conditions.

The cost of power not served due to cable failures was set to be 80 EUR per MWh [10], and the cost of power loss due to the wake effect was set to be 29.33 EUR per MWh [18,62]. Surface concession cost was set to be 0.17 EUR per meter squared in total capital cost [63,64]. Curves for other surface concession costs and wake-loss costs were also produced to test the robustness of the solution.

VI. Results

By comparing investment costs of the implemented layout to actual construction costs of the Barrow project [55], fixed construction costs across all layouts were approximated to be 162.59 MEUR. Most of these costs are related to turbine installation and turbine purchase. This adds 11.82 MEUR per year to the total investment cost of all layouts if annualized at a 4% interest rate over the 20-year life of the plant.

Given that no previous works had analyzed the impact of row distance and wake effect considering an optimal cable layout, we produced several curves to understand their dynamics. The results can be used to facilitate the design of large windfarms or, given that they provide insights on the energy benefits of using larger row distances, support surface concession negotiations at the earlier stages of a project.

Trials at 17 different scales of the Barrow layout were completed, such that at each configuration the turbine row spacing was 250m greater than the spacing of turbines within the row. A curve with exponential and linear components (Figure 1) was fit to the optimal objective function values at each spacing regime, which was then used to calculate an optimal turbine row spacing of approximately 1260 meters. A detailed comparison of the objective functions for the optimal and implemented layouts is

presented in Table 1. Investment cost and surface concession cost increased slightly in the optimal layout (0.16 and 0.10 MEUR per year respectively), while the wake cost decreased by 0.55 MEUR per year. In addition, four distance regimes were then optimized simultaneously to test the functionality of the model. The distance closest to optimal was correctly selected.

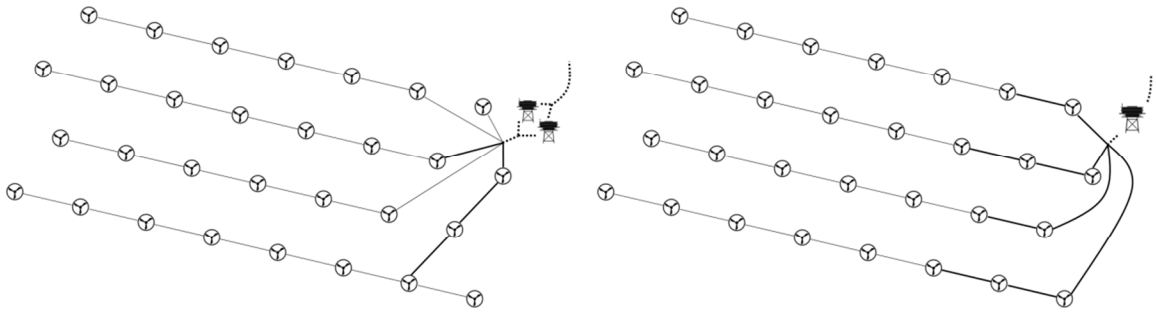

Figure 1. Optimal layout (left) compared to implemented layout (right). Rows in optimal layout are 1,260 meters apart, and turbines are spaced 1,010 meters apart compared to 750 and 500 respectively. The optimal layout contains a redundant offshore substation.

Investment cost and wake cost across the optimal layouts were also fit to curves. The investment cost (Figure 2) had a linear fit (R-squared 0.9976), and the wake cost had an exponential fit (R-squared 0.9999). This suggests that less computationally complex methods may suffice for determining optimal spacing of certain turbine layout regimes, especially for larger windfarms.

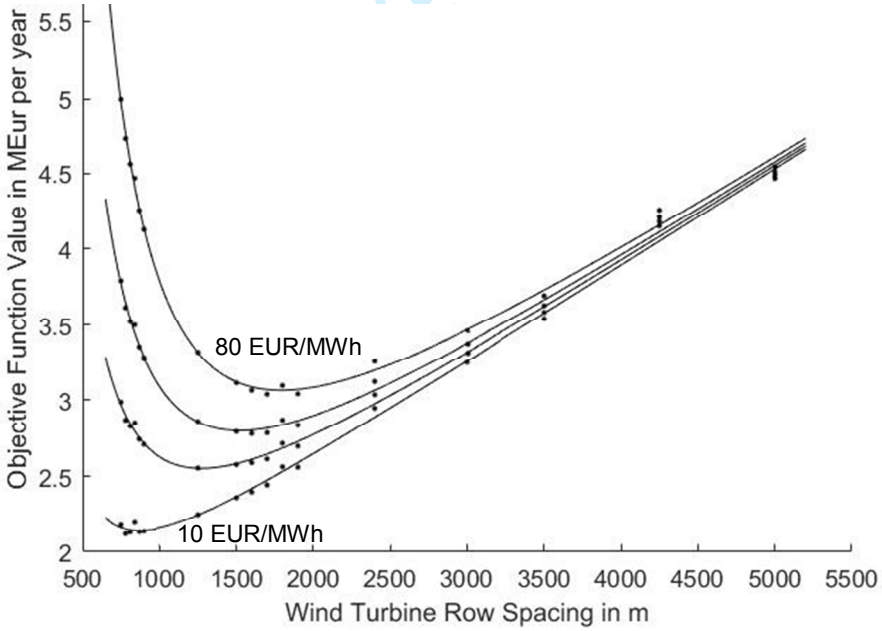

Figure 2. Comparison of optimal layout costs by wind turbine spacing given the alignment specified in Figure 1. Optimal wind turbine spacing increases as the cost of wake losses increases (10, 30, 50, and 80 EUR/MWh considered) [18,62].

The increases in investment cost should be approximately affine because most utilized connections have a linear increase in length and do not increase in capacity or redundancy in the range considered. The exponential fit of wake cost is most likely caused by the power curves of V90 turbines. Power not served varied more, but could possibly fit an inverse quadratic (R-squared 0.9844). Although more work must be

done to validate these models, they could be a useful tool to simplify the planning stage, which can be especially daunting in the case of larger windfarms.

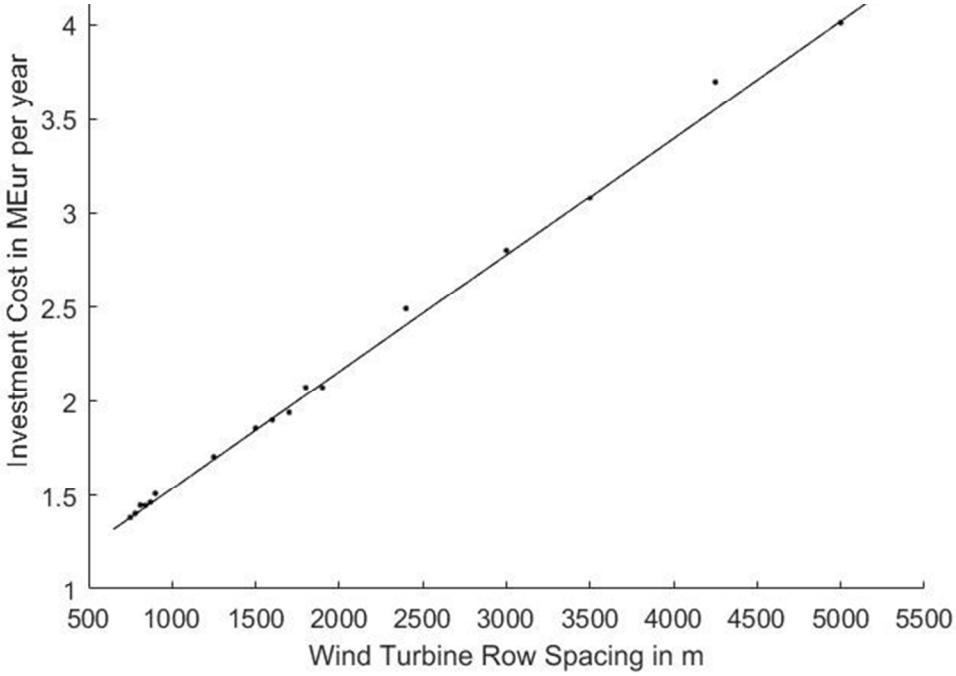

Figure 3. Comparison of optimal investment costs by wind turbine spacing given the alignment specified in Figure 1. Points are from 17 trials of the OWL model.

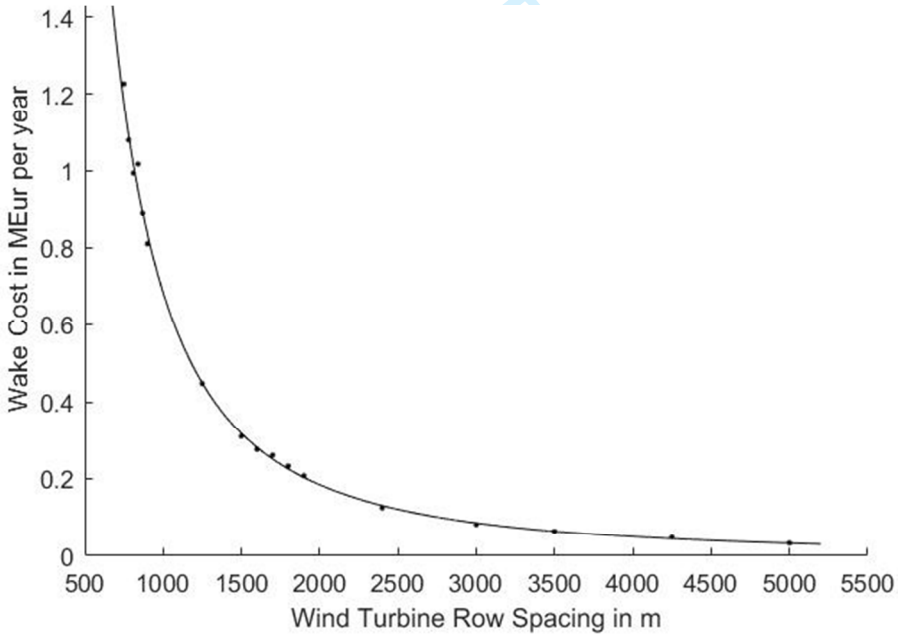

Figure 4. Comparison of wake costs by wind turbine spacing given the alignment specified in Figure 1. Points are from 17 trials of the OWL model.

VII. Conclusions

Continued interest in offshore windfarm investment has led to an increased importance of taking full advantage of optimal windfarm layouts. While investment cost may be modelled linearly, the interaction of power not served under cable failure in conjunction with the wake effect is difficult to model. This calls for concurrent optimization rather than model approximations to account for electrical layout costs during turbine placement optimization.

The Extended OWL model presented in this paper optimizes turbine spacing and electrical layout decisions, such that the resulting windfarm layout described is optimal based on the turbine placement schemes considered. The model uses MILP to concurrently optimize turbine positioning and cable layout. It relies on Jensen's approximation to deal with the wake effects, which are calibrated using years of mast data.

The model has been applied to Barrow Offshore Windfarm, an existing wind farm, to assess its potential savings. The optimal solution found by Extended OWL improves the implemented layout by 440,000 EUR per year, or 8.8 MEUR over the life of the plant. This is a calculated 10% savings of combined power not served, surface concession, wake, and cable costs. The designs are very different with respect to turbine spacing despite maintaining the same alignment. The optimal solution found was in line with studies that dealt with optimal turbine spacing alone. However, there could be surface concession constraints at the planning stage of BOWF that could have led to a tighter-than-optimal design.

The model can also develop curves that represent objective function value as a function of layout scale for each alignment regime. These curves can be used to compare conventional and unconventional turbine placement schemes and assess design tradeoffs. These curves can also be used for surface concession negotiations or layout planning depending on the stage of the project. If surface concession costs have already been negotiated, the model can incorporate post-negotiation representations of surface concession costs associated with each turbine layout.

The resulting model is robust with respect to the main factors affecting the problem, and can also directly compare layouts of completely different turbine placement schemes simultaneously. Such comprehensive modeling is essential to optimally account for tradeoffs that can be worth millions of euros in a single offshore project.

Funding Information--Support for the first and last authors was provided by the US National Science Foundation, WINDINSPIRE Grant OISE 1243482.

VIII. References

1. Rogelj J, Den Elzen M, Höhne N, et al. Paris agreement climate proposals need a boost to keep warming well below 2 C. *Nature*. 2016;534(7609):631-639.

2. Roadmap E. 2050: A practical guide to a prosperous, low carbon europe. *Brussels: ECF*. 2010.

3. Ho A, Mbistrova A. The european offshore wind industry-key trends and statistics 1st half 2015. *A report by the European Wind Energy Association*-. 2015.

4. Investment-grade climate policy: The next phase for europe. . 2015.

5. Mbistrova A. Financing and investment trends. *The European Wind Industry in 2016*. 2017.

6. Schwartz M, Heimiller D, Haymes S, Musial W. *Assessment of offshore wind energy resources for the United States*. 2010.

7. Breton S, Moe G. Status, plans and technologies for offshore wind turbines in europe and north america. *Renewable Energy*. 2009;34(3):646-654.

8. Allison TD, Jedrey E, Perkins S. Avian issues for offshore wind development. *Mar Technol Soc J*. 2008;42(2):28-38.

9. Punt MJ, Groeneveld RA, Van Ierland EC, Stel JH. Spatial planning of offshore wind farms: A windfall to marine environmental protection? *Ecol Econ*. 2009;69(1):93-103.

10. Lumbreras S, Ramos A. Optimal design of the electrical layout of an offshore wind farm applying decomposition strategies. *IEEE Trans Power Syst*. 2013;28(2):1434-1441.

11. Lundberg S. *Wind farm configuration and energy efficiency studies: Series DC versus AC layouts.* Chalmers University of Technology; 2006.

12. Lundberg S. Evaluation of wind farm layouts. *Epe journal*. 2006;16(1):14-21.

13. Quinonez-Varela G, Ault G, Anaya-Lara O, McDonald J. Electrical collector system options for large offshore wind farms. *IET Renewable Power Generation*. 2007;1(2):107-114.

14. Bozelie J, Pierik J, Bauer P, Pavlovsky M. DOWEC grid failure and availability calculation. *NEG Micon, Bunnik*. 2002;2.

15. Wiggelinkhuizen E, Verbruggen T, Braam H, et al. CONMOW: Condition monitoring for offshore wind farms. . 2007:118-122.

16. Tran R, Wu J, Denison C, Ackling T, Wagner M, Neumann F. Fast and effective multi-objective optimisation of wind turbine placement. . 2013:1381-1388.

17. Szafron C. Offshore windfarm layout optimization. . 2010:542-545.

18. Katic I, Højstrup J, Jensen NO. A simple model for cluster efficiency. . 1986:407-410.

19. Hou P, Hu W, Soltani M, Chen Z. Optimized placement of wind turbines in large-scale offshore wind farm using particle swarm optimization algorithm. *IEEE Transactions on Sustainable Energy*. 2015;6(4):1272-1282.

20. Bilbao M, Alba E. Simulated annealing for optimization of wind farm annual profit. . 2009:1-5.

21. Rašuo BP, Bengin AČ. Optimization of wind farm layout. *FME Transactions*. 2010;38(3):107-114.

22. Donovan S. An improved mixed integer programming model for wind farm layout optimisation. . 2006:143-151.

23. Mustakerov I, Borissova D. Wind turbines type and number choice using combinatorial optimization. *Renewable Energy*. 2010;35(9):1887-1894.

24. Elkinton CN, Manwell JF, McGowan JG. Algorithms for offshore wind farm layout optimization. *Wind Eng*. 2008;32(1):67-84.

25. Şişbot S, Turgut Ö, Tunç M, Çamdalı Ü. Optimal positioning of wind turbines on gökçeada using multi□objective genetic algorithm. *Wind Energy*. 2010;13(4):297-306.

26. Mosetti G, Poloni C, Diviacco B. Optimization of wind turbine positioning in large windfarms by means of a genetic algorithm. *J Wind Eng Ind Aerodyn*. 1994;51(1):105-116.

27. Wan C, Wang J, Yang G, Zhang X. Optimal micro-siting of wind farms by particle swarm optimization. *Advances in swarm intelligence*. 2010:198-205.

28. Lumbreras S, Ramos A. Offshore wind farm electrical design: A perspective. *Wind Energy*. 2012;16:459-473.

29. Green J, Bowen A, Fingersh LJ, Wan Y. Electrical collection and transmission systems for offshore wind power. . 2007.

30. Prasai A, Yim J, Divan D, Bendre A, Sul S. A new architecture for offshore wind farms. *IEEE Transactions on Power Electronics*. 2008;23(3):1198-1204.

31. Lumbreras S, Ramos A. A benders' decomposition approach for optimizing the electric system of offshore wind farms. . 2011:1-8.

32. Huang H. Distributed genetic algorithm for optimization of wind farm annual profits. . 2007:1-6.

33. Elkinton CN, Manwell JF, McGowan JG. Offshore wind farm layout optimization (owflo) project: An introduction. *Offshore Wind*. 2005:1-9.

34. Zhao M, Chen Z, Blaabjerg F. Generation ratio availability assessment of electrical systems for offshore wind farms. *IEEE Trans Energy Convers*. 2007;22(3):755-763.

35. Zhao M, Chen Z, Blaabjerg F. Optimisation of electrical system for offshore wind farms via genetic algorithm. *IET Renewable Power Generation*. 2009;3(2):205-216.

36. Banzo M, Ramos A. Stochastic optimization model for electric power system planning of offshore wind farms. *IEEE Trans Power Syst*. 2011;26(3):1338-1348.

37. Negra NB, Holmstrom O, Bak-Jensen B, Sorensen P. Aspects of relevance in offshore wind farm reliability assessment. *IEEE Trans Energy Convers*. 2007;22(1):159-166.

38. Sannino A, Breder H, Nielsen EK. Reliability of collection grids for large offshore wind parks. . 2006:1-6.

39. González JS, Rodríguez AG, Mora JC, Santos JR, Payán MB. A new tool for wind farm optimal design. . 2009:1-7.

40. da Silva FF, Castro R. Power flow analysis of HVAC and HVDC transmission systems for offshore wind parks. *International Journal of Emerging Electric Power Systems*. 2009;10(3).

41. Bresesti P, Kling WL, Hendriks RL, Vailati R. HVDC connection of offshore wind farms to the transmission system. *IEEE Trans Energy Convers*. 2007;22(1):37-43.

42. Global offshore wind farm database. www.4coffshore.com/offshorewind/.

43. Teodorescu, F Blaabjerg Z Chen R, Iov F. Power electronics in wind turbine systems. . 2006.

44. Lazaridis L. Economic comparison of HVAC and HVDCSolutions for large offshore wind farms underSpecial consideration of reliability. . 2005.

45. Tande J, Korpås M, Warland L, Uhlen K, Van Hulle F. Impact of TradeWind offshore wind power capacity scenarios on power flows in the european HV network. . 2008.

46. Rújula A, Martínez R. A new tool for the optimal design of electrical cables in wind farms. . 2005.

47. Li DD, He C, Fu Y. Optimization of internal electric connection system of large offshore wind farm with hybrid genetic and immune algorithm. . 2008:2476-2481.

48. Binato S, Pereira MVF, Granville S. A new benders decomposition approach to solve power transmission network design problems. *IEEE Trans Power Syst*. 2001;16(2):235-240.

49. Dutta S, Overbye T. A clustering based wind farm collector system cable layout design. . 2011:1-6.

50. Li DD, He C, Fu Y. Optimization of internal electric connection system of large offshore wind farm with hybrid genetic and immune algorithm. . 2008:2476-2481.

51. Peña A, Réthoré P, Laan MP. On the application of the jensen wake model using a turbulence□ dependent wake decay coefficient: The sexbierum case. *Wind Energy*. 2016;19(4):763-776.

52. Hartigan JA, Wong MA. Algorithm AS 136: A k-means clustering algorithm. *Journal of the Royal Statistical Society.Series C (Applied Statistics)*. 1979;28(1):100-108.

53. Billinton R, Chen H, Ghajar R. Time-series models for reliability evaluation of power systems including wind energy. *Microelectronics Reliability*. 1996;36(9):1253-1261.

54. Sánchez-Martín P, Ramos A, Alonso JF. Probabilistic midterm transmission planning in a liberalized market. *IEEE Trans Power Syst*. 2005;20(4):2135-2142.

55. Farm BOW. Offshore wind capital grants scheme. .

56. Barrow offshore wind farm post-construction monitoring report. . 2008:60.

57. Aarhus N. V90-3.0MW: A better wind business by design. . 2013.

58. The marine data exchange. www.marinedataexchange.co.uk/.

59. Niayifar A, Porté-Agel F. Analytical modeling of wind farms: A new approach for power prediction. *Energies*. 2016;9(9):741.

60. Hasager CB, Rasmussen L, Peña A, Jensen LE, Réthoré P. Wind farm wake: The horns rev photo case. *Energies*. 2013;6(2):696-716.

61. Stevens RJ, Gayme DF, Meneveau C. Generalized coupled wake boundary layer model: Applications and comparisons with field and LES data for two wind farms. *Wind Energy*. 2016;19(11):2023-2040.

62. Rivas RA, Clausen J, Hansen KS, Jensen LE. Solving the turbine positioning problem for large offshore wind farms by simulated annealing. *Wind Eng*. 2009;33(3):287-297.

63. Stevens RJ, Hobbs BF, Ramos A, Meneveau C. Combining economic and fluid dynamic models to determine the optimal spacing in very large wind farms. *Wind Energy*. 2017;20(3):465-477.

64. Tweed K. Statoil wins NY offshore wind rights for $42M. . . Available from: www.greentechmedia.com/articles/read/statoil-wins-ny-offshore-wind-rights-for-42m.

IX. TABLES

	Total Cost	Investment Cost	Wake Cost	Power Not Served Cost	Surface Concession Cost
Implemented Layout	3.08	1.40	1.18	0.39	0.11
Optimized Layout	2.78	1.56	0.63	0.38	0.21

Table 1. Comparison of the optimal layout objective function to the implemented layout objective function in MEUR per year.

X. Bibliographies

Thomas Marge is studying to receive a M.S.E. and B. S. in Applied Mathematics as well as a B.S. in Mathematics from the Johns Hopkins University in May 2018. His current areas of interest include optimization and renewable energies.

Sara Lumbreras Sara Lumbreras holds a PhD and a MSc Eng from Universidad Pontificia Comillas. She is an assistant professor at the Institute for Research in Technology and teaches at the Industrial Management Department at the ICAI School of Engineering and the Financial department at the ICADE School of Business and Law. Her research focuses on the development and application of decision support techniques for complex problems, mainly in the energy sector and in particular in grid design. She specializes in stochastic optimization (classical and based on metaheuristics) and in risk management.